Journal of Experimental Botany, Vol. 63, No. 8, pp. 3229–3241, 2012
doi:10.1093/jxb/ers047 Advance Access publication 29 February, 2012
This paper is available online free of all access charges (see http://jxb.oxfordjournals.org/open_access.html for further details)

Journal of Experimental Botany
www.jxb.oxfordjournals.org

RESEARCH PAPER

Sporophytic ovule tissues modulate the initiation and progression of apomixis in *Hieracium*

Matthew R. Tucker[1,*], Takashi Okada[1], Susan D. Johnson[1], Fumio Takaiwa[2] and Anna M. G. Koltunow[1,†]

[1] CSIRO Plant Industry, Waite Campus, Hartley Grove, Urrbrae SA 5064, Australia
[2] Transgenic Crop Research and Development Centre, National Institute of Agrobiological Sciences, Tsukuba, Ibaraki, Japan

* Present address: ARC Centre of Excellence in Plant Cell Walls, University of Adelaide, Waite Campus, Urrbrae, SA 5064, Australia.
† To whom correspondence should be addressed. E-mail: anna.koltunow@csiro.au

Received 29 July 2011; Revised 30 January 2012; Accepted 31 January 2012

Abstract

Apomixis in *Hieracium* subgenus *Pilosella* initiates in ovules when sporophytic cells termed aposporous initial (AI) cells enlarge near sexual cells undergoing meiosis. AI cells displace the sexual structures and divide by mitosis to form unreduced embryo sac(s) without meiosis (apomeiosis) that initiate fertilization-independent embryo and endosperm development. In some *Hieracium* subgenus *Pilosella* species, these events are controlled by the dominant *LOSS OF APOMEIOSIS* (*LOA*) and *LOSS OF PARTHENOGENESIS* (*LOP*) loci. In *H. praealtum* and *H. piloselloides*, which both contain the same core *LOA* locus, the timing and frequency of AI cell formation is altered in derived mutants exhibiting abnormal funiculus growth and in transgenic plants expressing *rolB* which alters cellular sensitivity to auxin. The impact on apomictic and sexual reproduction was examined here when a chimeric *RNAse* gene was targeted to the funiculus and basal portions of the ovule, and also when polar auxin transport was inhibited during ovule development following *N*-1-naphthylphthalamic acid (NPA) application. Both treatments led to ovule deformity in the funiculus and distal parts of the ovule and *LOA*-dependent alterations in the timing, position, and frequency of AI cell formation. In the case of NPA treatment, this correlated with increased expression of DR5:GFP in the ovule, which marks the accumulation of the plant hormone auxin. Our results show that sporophytic information potentiated by funiculus growth and polar auxin transport influences ovule development, the initiation of apomixis, and the progression of embryo sac development in *Hieracium.* Signals associated with ovule pattern formation and auxin distribution or perception may influence the capacity of sporophytic ovule cells to respond to *LOA*.

Key words: Apomixis, auxin, gametophyte, ovule, seed.

Introduction

Seed development in flowering plants requires the initiation of floral development and the formation of anthers and ovules. Within these organs, sporophytic reproductive precursor cells undergo meiotic reduction and then mitosis to give rise to the male pollen grain containing two sperm cells and a multi-cellular female gametophyte (embryo sac). During double fertilization in the ovule, one sperm nucleus fuses with the egg cell to give rise to the embryo and the other with the central cell to produce the endosperm, thus forming the two major constituents of the mature seed.

The ovule is possibly the most vital structure involved in seed development. It is physically connected to the maternal ovary tissues of the plant that supply hormones and nutrients via the funiculus, and incorporates specific tissues called the integuments that form the seed coat and protect the seed during its development (reviewed in Gasser *et al.*, 1998; Yang *et al.*, 2010). A third region in the ovule, the nucellus, supports growth of the embryo sac, which houses the egg cell and central cell and eventually the embryo and endosperm (Chaudhury *et al.*, 2001). Different regions

of the ovule are critical for normal gamete formation and seed development. For example, mutations in the *Arabidopsis SPOROCYTELESS/NOZZLE* gene induce cell-fate changes in the nucellus and prevent differentiation of the megaspore mother cell, which is the progenitor cell of the embryo sac (Yang *et al.*, 1999; Balasubramanian and Schneitz, 2000). The epidermal layer of the *Arabidopsis* nucellus also plays a specific role via endogenous small RNA pathways to regulate the fate and number of sub-epidermal cells entering the gametophytic pathway (Olmedo-Monfil *et al.*, 2010). Furthermore, alterations in the level or distribution of phytohormones such as auxin and ethylene (De Martinis and Mariani, 1999; Pagnussat *et al.*, 2009), and mutations in transcription factors that compromise integument growth such as *BEL1* (Reiser *et al.*, 1995), *WUSCHEL* (Gross-Hardt *et al.*, 2002), and *INNER NO OUTER* (Villanueva *et al.*, 1999) also lead to defects in embryo sac development. Collectively, these findings suggest that development of the embryo sac is sensitive to multiple positional inputs from the surrounding sporophytic ovule tissues (Gasser *et al.*, 1998; Bencivenga *et al.*, 2011).

Alterations in positional information within the ovule are also likely to influence the initiation and efficiency of asexual reproductive processes such as apomixis (Koltunow and Grossniklaus, 2003; Curtis and Grossniklaus, 2007; Tucker and Koltunow, 2009). In apomictic *Hieracium* subgenus *Pilosella* species that undergo the apospory type of apomixis, sexual reproduction initiates first with the differentiation of a megaspore mother cell that undergoes meiosis (Fig. 1A) to produce a tetrad of megaspores (Figs 1A, 2A, B; Koltunow *et al.*, 1998*b*). However, these meiotic products are displaced by adjoining sporophytic cell(s) called aposporous initial (AI) cells that bypass meiosis (apomeiosis), initiate mitosis (Figs 1A, 2C) and produce an embryo sac containing cells resembling the sexual egg and central cell. Embryo and endosperm development subsequently initiate in the absence of fertilization (Fig. 2D; Koltunow *et al.*, 1998*b*, 2000).

Genetic studies in aneuploid *H. praealtum* (R35) and analyses of apomixis mutants suggest that the two components of apomixis in *Hieracium*, apomeiosis and autonomous seed development, are controlled by two independent dominant loci, *LOSS OF APOMEIOSIS* (*LOA*) and *LOSS OF PARTHENOGENESIS* (*LOP*), respectively (Catanach *et al.*, 2006). Furthermore, a recent study showed that the core *LOA* locus in R35 is highly conserved in tetraploid *H. caespitosum* (C36), tetraploid *H. piloselloides* (D36), and diploid *H. piloselloides* (D18; Okada *et al.*, 2011). Analysis of these and other *Hieracium* species showed that the details of the mechanism of apospory, such as the timing and frequency of AI cell initiation or the type of embryo sac growth, can vary between plants and/or sub-species (Koltunow *et al.*, 2000, 2011). In the case of D18, a higher frequency of early AI differentiation and ectopic embryo formation in integument tissues appeared to correlate with abnormal ovule twisting and defective funiculus development compared with its parental line, D36 (Koltunow *et al.*, 2000). Changes in the frequency and location of AI cells were also observed in deformed ovules from R35 gamma irradiation mutants carrying deletions in unknown regions outside the *LOA* locus (Koltunow *et al.*, 2011) and in D36 plants expressing the *rolB* oncogene from *Agrobacterium rhizogenes*, which increases cellular sensitivity to the phytohormone auxin (Koltunow *et al.*, 2001). Auxin is known to play diverse roles in plant growth and morphogenesis including gynoecium morphogenesis, female gametophyte development, and embryo patterning (Nemhauser *et al.*,

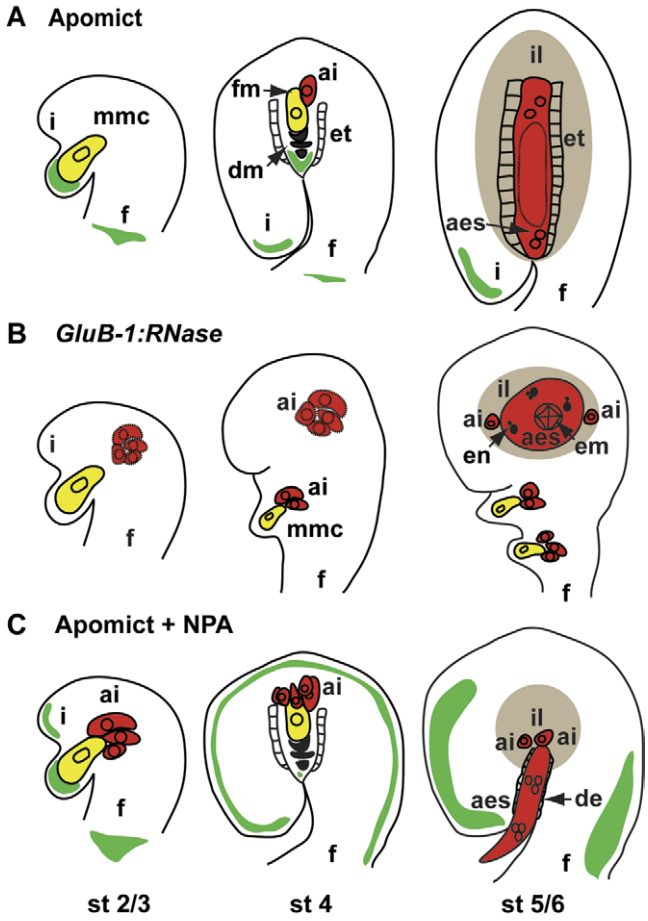

Fig. 1. Schematic representation of ovule development in wild-type, *GluB-1:RNase*, and NPA-treated apomictic *Hieracium* plants. (A–C) Comparison of early stages of ovule development, including megaspore mother cell initiation, megaspore selection, aposporous initial cell differentiation, and early embryo sac development in (A) untransformed apomictic *Hieracium*, (B) transgenic *GluB1:RNase* apomictic *Hieracium*, and (C) NPA-treated apomictic *Hieracium*. Yellow shading indicates sexual structures, red shading highlights apomictic structures, grey shading highlights regions of integument liquefaction, and green shading indicates the approximate localization of DR5:GFP expression. Ovule stage numbers are indicated at the bottom of the figure. Abbreviations: i, integument; mmc, megaspore mother cell; f, funiculus; fm, functional megaspore; ai, aposporous initial cell; dm, degenerating megaspores; et, endothelium; il, integument liquefaction; aes, aposporous embryo sac; en, endosperm; em, embryo; de, degenerating endothelium.

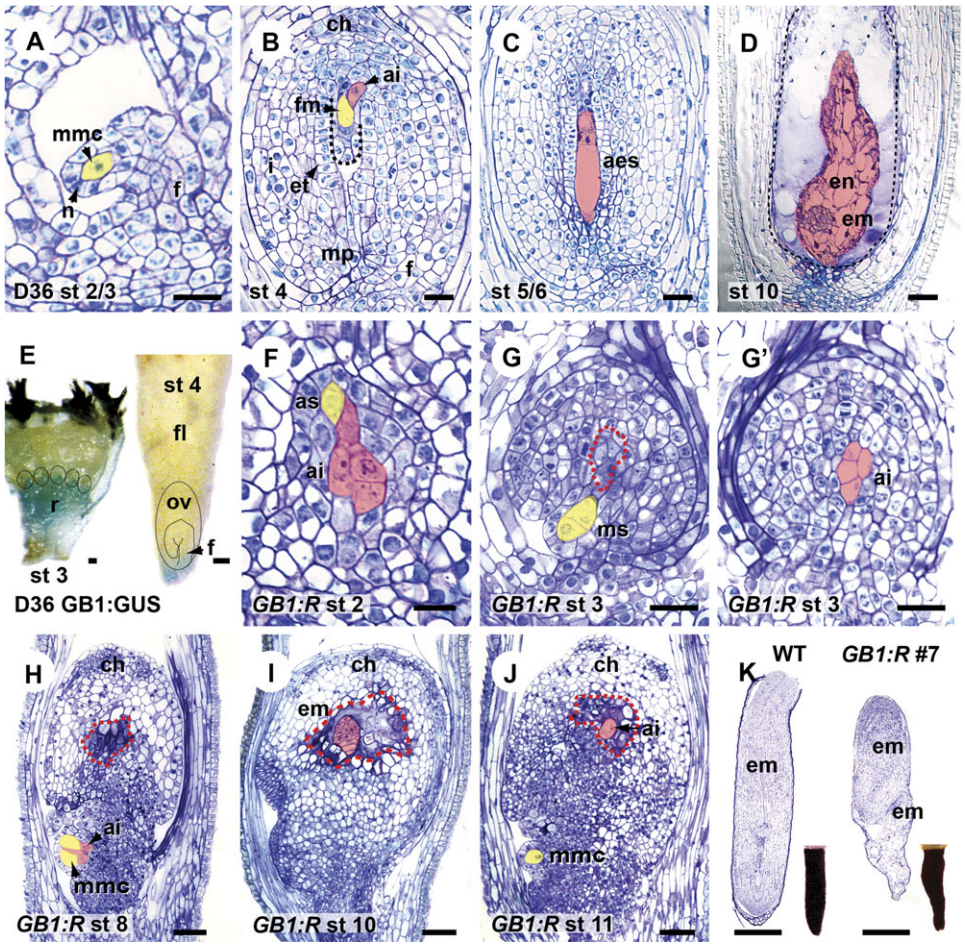

Fig. 2. *GluB-1:RNase* leads to a de-regulation of apomixis in *Hieracium*. (A–D) Sections of ovules from untransformed D36 *Hieracium* stained with Toluidine Blue. (A) Young ovule initiating sexual reproduction. (B) Ovule containing an aposporous initial cell displacing the sexual megaspore tetrad. The chalazal and micropylar orientation of the ovule is indicated. (C) Ovule showing an aposporous embryo sac undergoing mitosis. (D) Seed containing an embryo and endosperm. (E) GluB-1:GUS in a stage 3 capitulum and a stage 4 floret from *Hieracium* D36. The blue staining indicates expression and the dashed rings indicate the position of the ovaries. (F–J) Ovule sections from D36 *GluB-1:RNase* line #7 stained with Toluidine Blue. (F) Young ovule containing an archesporial cell and precocious aposporous initial-like cells. (G–G') Ovule showing megaspores and multiple expanding AI-like cells in different planes via serial sections. The red dashed line indicates the approximate position of the aposporous initial cells in subsequent sections relative to the sexual structures. (H) Ovule containing aborted megaspore mother cells and aposporous initials at the micropylar end of the ovule and an enlarged outgrowth at the chalazal end. (I) Ovule showing a chalazal embryo forming in the apparent absence of endosperm. (J) Ovule showing an aborted megaspore mother cell and chalazal aposporous initial cell. (K) Section of a mature seed containing a single embryo from D36 and a constricted seed from D36 *GluB-1:RNase* line #7. The whole mature seeds are also shown. Dashed red lines in (H)–(J) indicate regions of integumentary liquefaction. Yellow false colouring indicates cells acting in the sexual pathway, pink false colouring indicates cells acting in the apomictic pathway. Stages of ovule development are indicated in each panel. Abbreviations: aes, aposporous embryo sac; as, archesporial cell; ai, aposporous initial cell; em, embryo; en, endosperm; et, endothelium; f, funiculus; fl, floret; fm, functional megaspore; GB1:GUS, GluB-1:GUS; GB1:R, *GluB-1:RNase*; i, integument; ov, ovary; mmc, megaspore mother cell; mp, micropyle; ms, megaspores; n, nucellar lobe; r, receptacle; st, stage. Bar=50 μm in (D) and (E), 300 μm in (K), and 20 μm in all other panels.

2000; Weijers *et al.*, 2006; Pagnussat *et al.*, 2009). In *Hieracium 35S:rolB* plants it was unclear if the observed effects on altered apomictic initiation resulted from *rolB* influencing cellular responses to auxin, or from the alterations in cell signalling caused by dramatic changes in ovule morphology that were induced because of constitutive *rolB* expression (Koltunow *et al.*, 2001).

In this study, the influence of ovule tissues on apomixis in *Hieracium* was investigated by targeting the ablation of funicular cells and altering ovule auxin levels by applying an inhibitor of polar auxin transport. The treatments were assessed by cytologically examining the effects on ovule development and apomixis. The results suggest that information from sporophytic tissues, involving pathways dependent upon funiculus development and the phytohormone auxin, acts in parallel or upstream of the dominant *LOA* locus to influence the timing and progression of the apomictic process in *Hieracium*.

Materials and methods

Plant material

Plants used in this study were maintained by vegetative propagation and grown in greenhouses under the same conditions as described previously (Koltunow *et al.*, 1998*b*). Plant materials were chosen based on the fact they have been described previously and extensively characterized via cytological methods (Koltunow *et al.*, 1998*b*, 2000, 2011; Okada *et al.*, 2011), and because they contained the same core *LOA* locus (Okada *et al.*, 2011). Self-incompatible, facultatively apomictic *Hieracium piloselloides* (tetraploid D36 and diploid D18) and *H. praealtum* (aneuploid R35) produce >95% of seed via apospory coupled with autonomous seed formation, while *H. pilosella* (tetraploid P36; $4x=2n=36$) is a self-incompatible, obligate sexual plant that requires cross-pollination to produce seed (Koltunow *et al.*, 1998*b*, 2000, 2011; Okada *et al.*, 2011). D18 ($2x=2n=18$) was derived from D36 ($4x=2n=36$) by autonomous embryogenesis of a rare meiotically reduced egg (Koltunow *et al.*, 2011). The isolation and characterization of R35 ($3x+8=2n=35$) gamma deletion mutants was described previously (Catanach *et al.*, 2006). The stages of floral development for *Hieracium* were used as a reference for staged tissue collections (Koltunow *et al.*, 1998*b*).

Transgenes and transformation

To determine the suitability of the rice glutellin seed storage protein B1 promoter (*GluB-1*) for funicular tissue ablation, a construct containing 1.3 kb of the *GluB-1* promoter inserted upstream of the beta-glucuronidase (*GUS*) gene was transformed into *Hieracium* using the plant transformation vector pBI121. The *GluB-1:RNase* gene was made by inserting the 1.3 kb *GluB-1* promoter fragment into a previously described *CG1:RNase* construct (Koltunow *et al.*, 1998*a*) in place of the *CG1* promoter. The *DR5:GFP* construct has previously been used as a marker for auxin accumulation (Ulmasov *et al.*, 1997; Dorcey *et al.*, 2009) and was a gift from Dolf Weijers. The *AtARF8:GUS* construct was described previously (Goetz *et al.*, 2006) and contains 1.8 kb of the 5′ upstream promoter sequence from the *Arabidopsis ARF8* gene fused to *GUS*. Constructs were electroporated into *Agrobacterium* strains LBA4404 or AGL1 for plant transformation by a floral disc method (Bicknell and Borst, 1994). PCR and Southern blot analyses were used to confirm the presence, integrity, and number of inserted genes in the kanamycin-resistant plants.

The self-incompatible nature, high hemizygosity, and high apomictic seed set (>95%) of apomictic *Hieracium* plants makes it almost impossible to generate true-breeding, homozygous transgenic apomictic lines. Similarly, crosses between apomictic and sexual *Hieracium* give rise to highly diverse progeny that are not directly comparable for assessing the effect of transgenes (Koltunow *et al.*, 2000). Therefore, for experimental consistency, primary transformed lines containing a single intact gene insertion from each species were selected for analysis (Koltunow *et al.*, 2000). The total number of primary lines examined for each gene was 5 for *GluB-1:GUS* in D36, 8 for *GluB-1:RNase* in D36, 8 for *GluB-1:RNase* in P36, 3 for *DR5:GFP* in R35, 3 for *DR5:GFP* in P36, 3 for *DR5:GFP* in *loalop* mutant 115, and 3 for *AtARF8:GUS* in D36. Analysis of GUS activity was carried out as described previously by Tucker *et al.* (2003).

Fluorescence analysis

Samples were examined for GFP expression on a Zeiss M1 Imager using filter set 42. Ovaries were dissected from staged florets in approximately 40 µl 10% glycerol on microscopy slides, and gently squashed with a glass cover slip to aid visualization of the ovule. A standard set of exposure times (500, 1000, 2000 ms) were used to capture each image via Axiovision software.

N-1-naphthylphthalamic acid (NPA) application

NPA (Alltech) was dissolved in DMSO and diluted to 0.01 mM, 0.1 mM, 1 mM, 10 mM, and 100 mM in 70% ethanol. In order to examine the effect of a pulse of NPA at different developmental stages, whole capitula containing 40–50 florets were dipped either before MMC formation (pre-stage 2) or before AI formation (late stage 3), left for 24 h and then rinsed in water. Ovules were collected at various times from the following day until the time of embryo sac formation. At least 10 capitula were dipped at each stage taking care not to use more than three capitula per plant and capitulum samples were pooled. The experiment was repeated twice. A total of 65 ovules were sectioned for analysis and at least 50 ovules per stage were examined for DR5:GFP.

Cytology

D36 *GluB-1:RNase* lines #7 and #34 and P36 *GluB-1:RNase* lines #3-1 and #7-3 were the most extensively examined in this study. Ovaries from all of the transgenic lines were fixed in FAA (50% ethanol, 10% formalin, 5% acetic acid) and cleared using methyl salicylate to examine a greater number of samples, as per Koltunow *et al.* (2011). Ovaries for serial sectioning were fixed in glutaraldehyde and embedded in Spurr's resin as described previously by Koltunow *et al.* (1998*b*). Approximately five ovules were sectioned per stage where possible. Sections and whole-mount ovules were examined using a Zeiss Axioplan microscope and digital images were collected using a Spot II camera. Figures were compiled using Adobe Photoshop and Illustrator software.

Results

Disruption of ovule funicular growth in apomictic Hieracium *leads to a de-regulation of apomixis during early ovule stages*

To impair communication between the ovule and other maternal tissues of the plant, a genetic cell ablation strategy was adopted that has previously been used to examine the relationships between cells and tissues during plant organ development (Mariani *et al.*, 1990; Beals and Goldberg, 1997; Koltunow *et al.*, 2011). These studies employed chimeric gene constructs consisting of characterized promoters to direct the activity of a linked ribonuclease gene in a spatially and temporally defined manner.

Studies in Citrus, tobacco, and rice detailed the GluB-1:GUS expression pattern during ovule and seed development (Takaiwa *et al.*, 1996; Koltunow *et al.*, 1998*a*; Wu *et al.*, 1998). In the *Hieracium* ovule, GluB-1:GUS was detected in the funiculus and the subtending ovary and receptacle cells at stages 2 and 3 when the ovules had differentiated a megaspore mother cell (Fig. 2E). In composite *Hieracium* flowers, the receptacle is the only point of contact between the individual florets and the floral capitulum. GluB-1:GUS persisted in stage 4 capitula when aposporous initial (AI) cells had differentiated in the ovules, but subsequently became confined to the base of the floret and the associated receptacle cells. Expression declined until the late stages of seed development when GUS expression was detected in the developing endosperm. The spatial and temporal dynamics of the *GluB-1* promoter in *Hieracium* suggested that it would be a useful tool to disrupt funiculus development and to impair communication between the

early ovule and surrounding tissues during the initiation of apomixis.

To maintain consistency between studies, apomictic *H. piloselloides* D36 was selected for transformation with the *GluB-1:RNase* construct. D36 typically initiates apomixis in a uniform manner, is sensitive to the activity of the *rolB* oncogene that induces changes in auxin sensitivity, and its derivative diploid plant D18 shows funicular defects (see Supplementary Fig. S1A–C at *JXB* online) and de-regulated apomixis (Koltunow *et al.*, 1998*b*, 2000, 2001). Sexual P36 was chosen as a non-apomictic control. In total, eight transgenic apomictic *H. piloselloides* D36 plants and eight transgenic sexual *H. pilosella* P36 plants were generated and all exhibited decreased seed set relative to the control lines. Two of the D36 plants and one P36 plant aborted capitulum and flower development at the very early stages and failed to initiate ovule or seed development (data not shown). In the remaining lines, flowers were viable and mature seeds were produced that had a distinctive terminal phenotype in that they were pointed and constricted at their site of attachment to the capitulum, reflecting the zone of expression of the ablation gene (Fig. 2K). Two D36 plants that produced seeds, #7 and #34, were selected for detailed histological analysis as they represented plants expressing the ablation gene at different levels from seed germination studies (Table 1). A further two P36 plants (#3-1 and #7-3), were also examined to provide a sexual control. The remaining lines were characterized in less detail but showed similar morphological and cytological phenotypes, suggesting that the phenotypes were due to the effects of the *GluB-1:RNase* transgene (data not shown).

In ovules from untransformed apomictic D36 plants, a single megaspore mother cell was observed at stage 2/3 (Fig. 2A) and an enlarged AI cell(s) was not apparent until stage 4 when meiosis was complete (Fig. 2B). One or two AI cells, distinguished by their large size, an enlarged central nucleus flanked by large vacuoles, and similarity to the functional megaspore, were usually detected in D36 ovules as per previous reports (Koltunow *et al.*, 1998*b*). In most ovules, one AI cell initiated embryo sac development and expanded to fill the space within the endothelium normally occupied by the sexual embryo sac by stage 5/6 (Fig. 2C). During subsequent stages, embryo and endosperm development initiated in the embryo sac (Fig. 2D), and continued until the embryo was fully mature and filled the elongated seed (Fig. 2K).

GluB-1:RNase line #7 in apomictic D36 *Hieracium* was the most strongly affected line since it produced only 16% viable seeds compared with 39% in line #34 and 60% in untransformed D36 (Table 1). Also, seeds from line #7 showed the strongest constriction and deformation at the point of connection to the receptacle (Fig. 2K). To characterize reproductive defects in lines #7 and #34, up to 10 ovules were serially sectioned per stage between stages 2 and 12, from ovule initiation to seed maturity. Distinct abnormalities were first observed during the early stages of ovule development. In contrast to untransformed D36, developing florets from *GluB-1:RNase* lines #7 and #34 showed small zones of necrosis and displaced zones of xylem formation at the base of the ovule funiculus (see Supplementary Fig. S2A, B, E–G at *JXB* online). Different degrees of reproductive abnormalities were observed in the two lines. In line #7, sexual processes aborted in most ovules during meiosis. Despite this, AI differentiation and expansion were prominent as early as archesporial cell initiation (Fig. 2F). Up to eight AI cells differentiated in ovules during the subsequent stages, and serial sections showed that these were spatially separated from the developing sexual cells in 50% (n=10) of cases (Fig. 2G–G'). Approximately 25% (n=20) of sectioned ovules aborted at this stage.

In line #34, ~13% (n=15) of the sectioned ovules had aborted at the early stages. In viable ovules, AI cells appeared at a similar stage compared to line #7, but with lower frequency and reduced displacement. One to three AIs were evident at the early stages in close proximity to the MMC (Fig. S2C–C') and only in ~10% (n=11) of cases were they spatially separated from sexual structures. The variations between lines #7 and #34 suggest that different doses of *GluB-1:RNase* function are contributing to the differences in ovule development and seed viability. In contrast to the transgenic D36 lines, only minimal effects were observed in the sexual P36 *GluB-1:RNase* plants during the early stages, where funiculus growth appeared to

Table 1. Seed formation and germination in *GluB-1:RNase* and untransformed *H. piloselloides* lines

Plant	Florets/capitulum[a]	No. of Seed heads	No. of seeds	Full seeds[b] set (%)	Germination rate (%)	
					4 d	30 d
D18	32±11	20	656	70	23±5	25±2
D36	33±6	10	343	84	34±8	60±5
D36 *GB1:R*[c] #7	33±13	70	2103	72	12±2	16±5
D36 *GB1:R* #30	33±3	5	166	70	45±6	52±3
D36 *GB1:R* #34	36±3	10	353	79	28±6	39±3
D36 *GB1:R* #37	33±3	10	326	81	37±3	45±3

[a] ± Values show standard deviation (SD) from replicate experiments.
[b] Full seeds indicates seeds that are large and black in colour compared to brown or white seeds that have aborted.
[c] *GluB-1:RNase*.

be abnormally elongated but no ectopic 'AI-like' cells could be detected in the ovule (data not shown). These results indicate that the integrity of funicular and receptacle tissues beneath the ovule influences the timing, frequency, and location of AI formation in apomictic D36.

GluB-1:RNase *induces polar nuclei defects, extra cell divisions and ectopic reproductive zones in ovules from apomictic* Hieracium

In the majority of ovules from the low expressing line #34, one of the early AI cells displaced the sexual structures and initiated mitosis at the micropylar end of the ovule. Apart from the early timing of AI formation, this was similar to D36 controls. However, during later developmental stages when the funicular region became more constricted, ovule growth occasionally appeared stunted and embryo sacs were observed containing small embryos without endosperm (see Supplementary Fig. S2D at *JXB* online). In 27% (n=15) of sectioned ovules from line #34, embryo sacs contained polar nuclei that had failed to divide. By contrast, quiescent polar nuclei were only observed in 1% of untransformed D36 samples at stage 8 (n=68). These data suggest that the reduced seed viability in line #34 is probably due to a combination of early ovule defects as well as failed endosperm development leading to embryo abortion.

In ovules from D36 *GluB-1:RNase* line #7 that progressed past the early stages, different classes of phenotypes were observed. In the minority of ovules, sporophytic cell divisions and growth were indistinguishable from untransformed D36 controls, but defects in polar nuclei division were observed similar to those in line #34. In others, the ovule integument recurved and formed a micropyle, and multiple aposporous structures continued development in the distal (chalazal) region of the ovule (see Supplementary Fig. S2G at *JXB* online). This contrasted with D36 and *GluB-1:RNase* line #34 where only one AI cell typically continued development closer to the micropyle (see Supplementary Fig. S2E, F at *JXB* online).

In the majority (60%, n=31) of ovules from *GluB-1:RNase* line #7, the funiculus became highly constricted and the endothelium and micropyle did not form (Fig. 2H–J; see Supplementary Fig. S2H–H' at *JXB* online). In these cases, somewhat surprisingly, ovule cells continued to divide resulting in the formation of chalazal outgrowths (Fig. 2H–J). Serial sections also showed the presence of multiple nucellar lobes containing both sexual and AI cells (see Supplementary Fig. S2H–H' at *JXB* online). Typically, the megaspores and the adjacent initials closer to the micropylar end of the ovule had aborted (Fig. 2H–J). However, cells in the chalazal region of the ovule continued dividing to form an enlarged dome where cell degeneration (liquefaction) occurred, indicating that the integumentary identity of the tissue had been retained (Fig. 2H–J; see Supplementary Fig. S2H–H' at *JXB* online). Apomictic processes occurred in such domes (Fig. 2I, J), spatially removed from the arrested sexual and AI cells by many cell layers. In some of these ovules, embryos formed in isolation surrounded by liquefying tissue (Fig. 2I; see Supplementary Fig. S2G at *JXB* online). In other ovules, AI cells (Fig. 2J) or inverted embryo sac structures containing egg-like cells (see Supplementary Fig. 2I at *JXB* online) and undivided polar nuclei were observed. Often a diverse array of structures including AI cells, cellular-like endosperm cells, embryos, and embryo sacs could be observed in the same ovule through serial sections. Such ovules resembled those described for *H. piloselloides* D18 (Koltunow *et al.*, 2000). The frequency of *GluB-1:RNase* line #7 ovules showing apomictic development in the integumentary domes and constriction at the micropylar end of the developing seed correlated with the mature fertile seed development shown in Fig. 2K. It is therefore likely that some of the viable seeds contained embryos derived from the chalazal zones. This is somewhat reminiscent of the multiple adventitious chalazal embryos that form from embryo initial cells in seeds from Citrus (Kobayashi *et al.*, 1979; Koltunow *et al.*, 1995).

Taken together, these observations suggest that the integrity of funicular and receptacle tissues in *Hieracium* is important for ovule development and apomixis, possibly because they transmit or synthesize regulatory information. Perturbations to these tissues in apomictic *GluB-1:RNase* D36 induced developmental changes in unconnected regions of the ovule, leading to abnormal integument growth, precocious differentiation of multiple AI cells and disorganized embryo sac development (Fig. 1B). Similar defects in funiculus growth may contribute to a de-regulation of apomixis in *H. piloselloides* D18 (see Supplementary Fig. S1 at *JXB* online; Koltunow *et al.*, 2000) and *H. praealtum* R35 deletion mutants (see Supplementary Fig. S1 at *JXB* online; Koltunow *et al.*, 2011), which produce extra and/or displaced AI cells as well as abnormal embryo sacs. These findings suggest that the capacity of sporophytic cells to respond to *LOA* and subsequently develop into embryo sacs is modulated by the surrounding tissues of the ovule not directly involved in the apomictic pathway.

Auxin maxima and auxin-responsive genes are detected in specific regions of the Hieracium *ovule, including the funiculus*

Previous studies in apomictic *Hieracium* D36 plants expressing the *rolB* oncogene suggested that alterations to auxin sensitivity in sporophytic tissues might contribute spatial and temporal control over the apomictic process (Koltunow *et al.*, 2001). In *Arabidopsis* ovules, auxin contributes to integument growth (Schruff *et al.*, 2006), embryo sac polarity (Pagnussat *et al.*, 2009), and vascular development (Ohashi-Ito *et al.*, 2010). Several approaches were used to determine if auxin signalling might be a sporophytic factor influencing ovule development and apomixis in *Hieracium*. Analysis of *AtARF8:GUS* in ovules from transgenic *Hieracium* D36 plants showed that GUS activity was detected predominantly in the funiculus at stage 4/5, and at later stages in the whole ovule as well as connective tissues of the receptacle (Fig. 3A, B). In *Arabidopsis*, *ARF8* is involved in

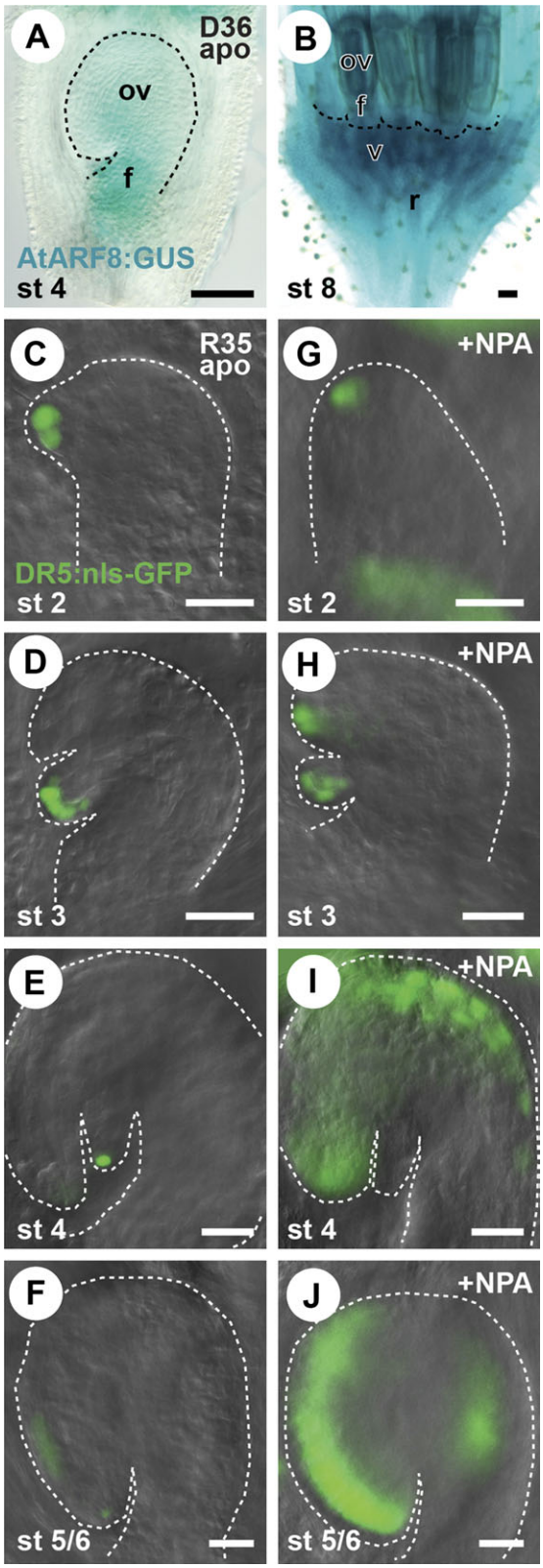

Fig. 3. AtARF8:GUS and DR5:GFP are detected in ovules from apomictic *Hieracium*. (A) AtARF8:GUS in a stage 4 D36 floret. The blue staining indicates expression and the dashed line indicates the position of the ovule. (B) AtARF8:GUS in a stage 8 D36 capitulum, showing strong staining in vascular tissues of the receptacle. (C–F) DR5:GFP accumulation in wholemount ovules from apomictic R35 capitula treated with 70% ethanol. (C) Young ovule showing nucellar outgrowth with GFP expression marked in green. (D) Ovule showing growth of the integument around the nucellar epidermis. (E) Ovule at the stage where meiosis is occurring and apomixis is initiating. (F) Mature ovule. (G–J) DR5:GFP accumulation in wholemount ovules from apomictic R35 capitula treated with 1 mM NPA in 70% ethanol. (G) Young ovule just prior to nucellar outgrowth. Increased levels of GFP are detected at the base of the ovule below the funiculus. (H) Ovule at a similar stage to (D) showing growth of the integument around the nucellar epidermis. GFP expression is detected at the tip of the nucellus and integument. (I) Ovule at a similar stage to (E) showing accumulation of GFP in the integument. (J) Ovule at a similar stage to (F) showing accumulation of GFP in the integument. Stages of ovule development are indicated in each panel. Dashed lines in (C)–(J) indicate the shape of the ovule. Abbreviations: apo, apomict, f, funiculus; ov, ovule; r, receptacle; v, vasculature. Bar=50 μm in (A) and (B) and 20 μm in all other panels.

mediating auxin responses and regulating the transcription of downstream genes (Goetz *et al.*, 2006).

Furthermore, DR5:GFP, which marks the sites of auxin accumulation in ovules (Dorcey *et al.*, 2009), was also detected during the early stages of *Hieracium* ovule development. In transgenic apomictic *H. praealtum* R35 (Fig. 3) and sexual P36 (see Supplementary Fig. S3 at *JXB* online) plants, DR5:GFP accumulated in one or a few cells at the distal tip of the young ovule (Fig. 3C; see Supplementary Fig. S3C at *JXB* online), apparently marking the juvenile nucellar epidermis prior to the appearance of the single integument. GFP was also detected in connective tissues directly below the funiculus of the ovule and in the receptacle (see Supplementary Fig. S3A at *JXB* online). During the events of MMC specification and meiosis, DR5:GFP expanded to include a pool of distal nucellar epidermal cells adjoining the reproductive cells (Fig. 3D), and in sexual P36 was also detected in the tip of the growing integument (see Supplementary Fig. S3D at *JXB* online). In later stages, no obvious GFP signal was detected in AI cells or enlarging embryo sacs in either species (Fig. 3E; see Supplementary Fig. S3E at *JXB* online). Expression subsequently diminished in the nucellar lobe but was detected in the tip of the integument (Fig. 3F; see Supplementary Fig. S3F at *JXB* online). Apart from the absence of DR5:GFP in the tip of the integument of young R35 ovules, patterns of GFP accumulation were very similar between sexual and apomictic *Hieracium*.

In summary, these results suggest that auxin accumulates in specific regions of the *Hieracium* ovule, including the tip of the nucellus, the tip of the integument, and the connective tissues located below the ovule funiculus (Fig. 1A). Based on this and the finding that *35S:rolB*, which increases auxin sensitivity, induces a de-regulation in apomixis somewhat similar to *Glub-1:RNase* (Koltunow *et al.*, 2001), it was considered that auxin accumulation or flow might contribute sporophytic information to the apomictic process.

Inhibition of polar auxin transport by NPA leads to alterations in flower development, seed viability, and accumulation of DR5:GFP

To examine the role of polar auxin transport during seed development in *Hieracium*, apomictic D36 capitula at late stage 3 were dipped in *N*-1-naphthylphthalamic acid (NPA) at concentrations varying from 0.01 mM to 100 mM (see Materials and methods), left to mature, and then the seeds were harvested for viability scoring and germination studies. NPA is a phytotropin that regulates auxin efflux and has previously been used to disrupt polar auxin transport and to characterize the effects on plant development (Reed *et al.*, 1998; Nemhauser *et al.*, 2000; Dorcey *et al.*, 2009).

The application of NPA had a pronounced effect on *Hieracium* flower development. Flower size and morphology were particularly sensitive to the inhibitor, with higher concentrations of NPA resulting in smaller florets that failed to open completely (Fig. 4A–C). Similarly, increasing concentrations of NPA had a dosage-dependent effect on seed viability and germination frequency (Fig. 4D). Approximately 82% (n=272) of the seeds produced by control plants treated with 70% ethanol appeared black in colour, typically a measure of viability, while the remainder were white or brown, indicative of early ovule or seed abortion. 79% of the black seeds germinated after 25 days on media. By contrast, only 42% (n=119) of the seeds produced after treatment with 10 mM NPA+70% ethanol appeared to be viable and only 2% germinated. The majority of seedlings from NPA-treated capitula germinated with extremely stunted roots (see Supplementary Fig. S4 at *JXB* online).

At lower concentrations of NPA, seed sterility was also increased relative to the wild-type control, but a higher proportion of seeds germinated compared with the 10 mM treatment (Fig. 4D). Application of 1 mM NPA led to changes in ovule DR5:GFP expression and similar effects were observed in all species examined. At the early stages of ovule outgrowth (stage 2), NPA caused DR5:GFP to accumulate to higher levels at the base of the ovule in cells adjoining the funiculus and the receptacle (Fig. 3G; see Supplementary Fig. S3B at *JXB* online). By stage 3, DR5:GFP accumulated at the tip of the integument, whereas in untreated plants it was either weak or absent (Fig. 3H). During subsequent stages, DR5:GFP was detected at high levels in the ovule, extending from the tip of the integument in a crescent shape towards the funiculus, following the path of integument growth (Fig. 3I, J). Strong accumulation of DR5:GFP in the integument indicates that auxin is apparently trapped within the ovule by NPA treatment, possibly through an inhibition of transport away from a site of synthesis at the tip of the integument, or through defects in the funiculus vasculature. Similar results were obtained in sexual P36 (see Supplementary Fig. S3 at *JXB* online).

Combined, these results show that polar auxin transport is important for flower and seed development in *Hieracium*. NPA has a dosage-dependent effect on seed viability in apomictic *Hieracium* and leads to changes in auxin accumulation during ovule development.

NPA treatment alters ovule development and the initiation of apomixis in Hieracium*, resulting in phenotypes similar to* GluB-1:RNase *plants*

To determine the effects of altering polar auxin transport during *Hieracium* ovule development, capitula were dipped in either 1 mM or 5 mM NPA before MMC formation (pre-stage 2) or before AI formation (late stage 3), left for 24 h, and then rinsed in water. Ovules were collected at subsequent stages until the time of embryo sac formation and were analysed by clearing or sectioning. The application of 5 mM NPA to pre-stage 2 capitula completely inhibited ovule growth in most florets (compare Fig. 4E with 4I), even though ovary growth continued normally. This indicates that polar auxin transport is required for ovule outgrowth in *Hieracium*, and seemingly explains the high sterility caused by high concentrations of NPA. The application of 1 mM NPA at the same stage did not inhibit ovule formation, however, allowing the effect of reduced polar auxin transport to be examined during subsequent stages of ovule development in apomictic plants.

In apomictic D36 capitula treated with 1 mM NPA prior to stage 2, the sexual process initiated and a megaspore mother cell (MMC) was observed in all ovules at stage 2/3 (Fig. 4J). However, in contrast to control plants (Fig. 4F), expansion of the MMC was accompanied by the appearance of multiple (2 or 3) AI-like cells at the chalazal end of the cell. The appearance of AI cell(s) was not detected in the control D36 plants until stage 4 (Fig. 4G), when meiosis was complete and megaspore selection was occurring. At stage 4/5, some NPA-treated ovules contained up to 10 AI cells in close proximity to the sexual structures (Fig. 4K). Many of the NPA-treated ovules appeared to be twisted relative to the plane of the ovary (Fig. 4M) as a result of alterations in funiculus and/or integument growth. By stage 6, most of the treated ovules were stunted (Fig. 4P) and cells in and around the endothelial layer were misshapen and/or heavily stained with toluidine blue, suggesting they were undergoing degradation. AI cells continued to differentiate in chalazal regions of the ovules throughout these stages with high frequency, but misshapen embryo sac structures were small and positioned close to the micropylar end of the ovule. Only 28% of the seeds produced after this treatment were capable of germinating (Fig. 4D).

Similarly, ovules from apomictic D36 capitula treated with 1 mM NPA at late stage 3 (after meiosis but prior to AI formation) showed developmental defects (Fig. 1C). In the majority of NPA-treated ovules at stage 4, multiple AI cells could be distinguished in chalazal regions adjoining megaspore tetrads. The most striking defects, however, were observed from stage 5 onwards. In many ovules, embryo sac(s) appeared to be extruded from the micropyle (Fig. 4L, N). In these cases, the embryo sac continued developing and dividing independent of its position away from the integument and ovule proper. At stage 6, the majority of treated ovules had failed to fill the space available within the ovary locule similar to the samples treated prior to stage 2 (Fig. 4P), and many displayed an abnormally stunted

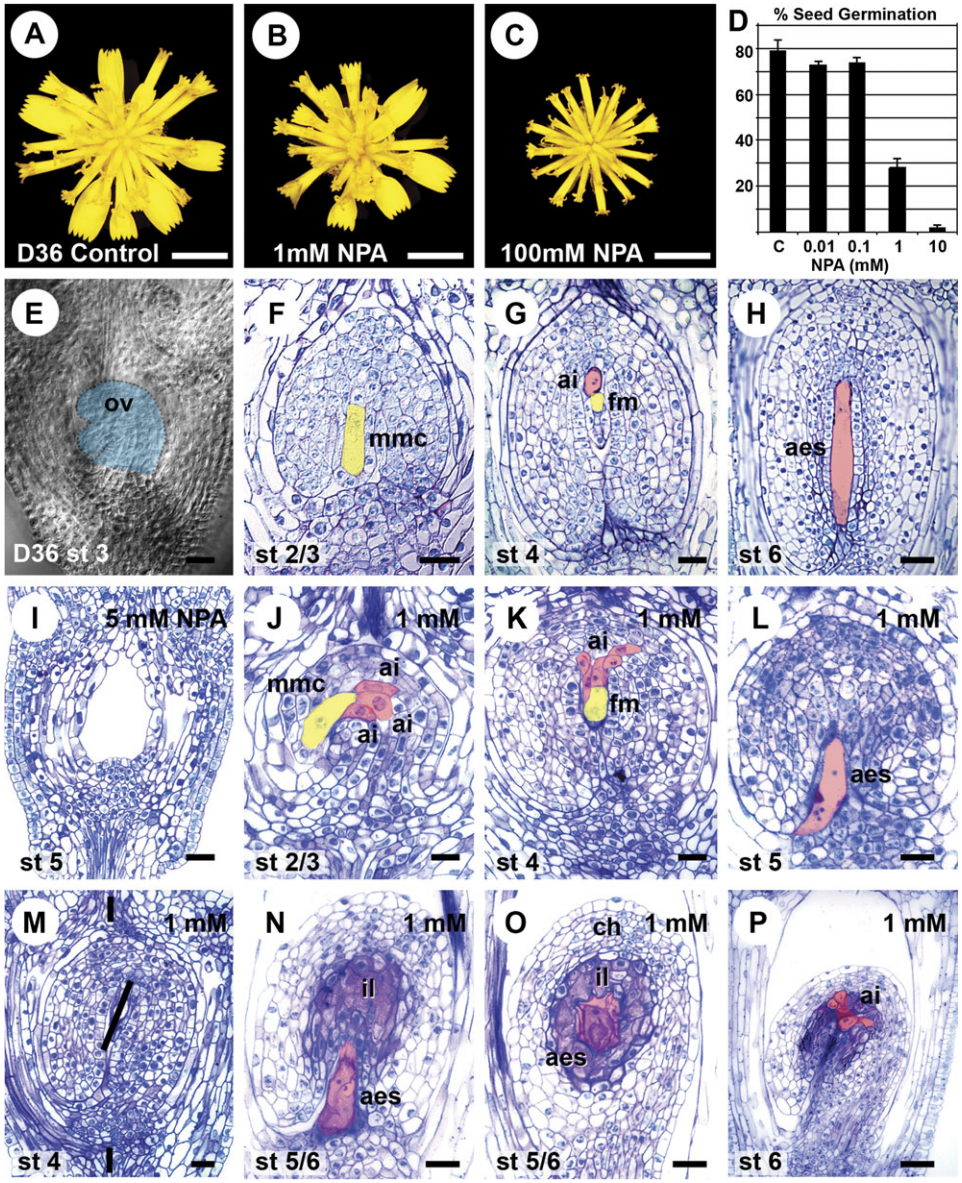

Fig. 4. NPA treatment alters flower development and the initiation of apomixis in D36 *Hieracium*. (A–C) D36 *Hieracium* flowers at stage 7 after treatment with different concentrations of NPA at stage 3. (D) Germination of seeds derived from capitula treated with different concentrations of NPA. (E–H) Ovules from apomictic D36 *Hieracium* florets treated with 70% ethanol. (E) Cleared wholemount stage 3 floret showing the position of the ovule (false coloured in blue) relative to surrounding ovary and floral tissues. (F) Ovule containing an MMC and no aposporous initial cells. (G) Ovule containing a single aposporous initial cell displacing the sexual functional megaspore. (H) Ovule showing an aposporous embryo sac undergoing mitosis. (I–P) Sections of ovules from NPA treated florets, dipped prior to stage 2 (I–K, P, M) or at stage 3 (L, N, O). (I) Empty locule of a 5 mM NPA-treated floret. (J) Two sections of a young ovule at a similar stage to (F) superimposed to show the megaspore mother cell and at least three aposporous initial cells. (K) Stunted ovule at a similar stage to (G) showing multiple aposporous initial cells differentiating in close proximity to the functional megaspore. (L) Stunted ovule containing a dividing embryo sac extruding through the micropyle. (M) NPA treatment twists ovule growth relative to the surrounding tissues, indicated by the line showing the skewed alignment. (N) Ovule at a similar stage to (H) showing an extruded cellularized embryo sac and integument liquefaction in the chalazal region. (O) Ovule at a similar stage to (H) showing development of an embryo sac surrounded by liquefying integumentary cells in the chalazal region. (P) Stunted ovule at a similar stage to (H) showing multiple aposporous events occurring in chalazal regions of the ovule. Yellow false colouring indicates cells acting in the sexual pathway, pink false colouring indicates cells acting in the apomictic pathway. Stages are indicated in each panel as are the concentrations of NPA used. Abbreviations: aes, aposporous embryo sac; ai, aposporous initial cell; C, control; ch, chalazal region; fm, functional megaspore; il, integument liquefaction; mmc, megaspore mother cell; ov, ovule; st, stage. Bar=5 mm in (A), (B), and (C) and 20 μm in all other panels.

funiculus. Multiple apomictic events initiated in the chalazal regions of the ovules, similar to the pre-stage 2 treated samples (Fig. 4O), forming displaced regions of degradation and AI initiation. These regions were similar to those observed in the *GluB-1:RNase* plants.

NPA is unable to stimulate AI differentiation in the absence of the LOA locus

To determine whether the appearance of extra AI-like cells in NPA-treated ovules was dependent upon the presence of the apomixis initiation locus (*LOA;* Catanach *et al.*, 2006), NPA treatments were repeated in sexual *Hieracium* P36 and in R35 *loalop* mutant 115 (m115), which both lack the capacity for AI formation and autonomous seed development. Analysis of DR5:GFP in P36 and m115 showed that polar auxin transport was inhibited by NPA in a similar manner to that in apomictic R35 (see Supplementary Fig. S4 at *JXB* online; data not shown). However, cytological analysis of ovules at stages 4, 6, and 10 failed to identify any ectopic AI-like cells or embryos in either background. In the absence of cross-pollination, no fertile seeds were set on either plant. This indicates that application of NPA is not sufficient to stimulate the formation of AI cells or embryos in *Hieracium* in the absence of the *LOA* locus.

Discussion

Sporophytic ovule tissues modulate the initiation of apomixis in Hieracium

In the search for the loci responsible for apomixis, little attention has been given to factors that impart temporal and spatial control on the reproductive process and thereby alter the plant's response to key loci such as *LOA*. In this study, the relationship between sporophytic tissues and the initiation of apomixis was examined in *Hieracium*. The aim was to determine whether the apomictic process is influenced by sporophytic information external to the reproductive cells, and if so, what aspects are susceptible. To achieve this, an ablation strategy was utilized to compromise communication between the ovule, the funiculus, and the receptacle, which forms the base of the floral capitulum and connects the female reproductive tissues to the rest of the plant. Transgenic *GluB-1:RNase* lines showed varying degrees of connective tissue ablation that, somewhat predictably, resulted in the abortion of flower and ovule development in extreme cases. However, in less severe cases, the ovules were viable and disruption of the connective tissues correlated with the precocious appearance of multiple AI-like cells in apomictic plants. Unlike control apomicts, these AI cells often formed prior to female meiosis and in isolated regions of the ovule, several cell layers away from the sexual cells. The differentiation of AI cells away from sexual cells is not typical of apomixis in *Hieracium*, but has been described in a previously characterized *Hieracium* mutant (*loa1*; Okada *et al.*, 2007). In *loa1* ovules, 'AI-like' cells differentiate several cell layers away from the meiotic tetrad, grow towards the funiculus, and fail to initiate mitosis. The AI cells in *GluB-1:RNase* are somewhat distinct from those in *loa1*, since they differentiate further away from the sexual cells, at higher frequency and appear to retain some capacity for further development. Higher frequencies of AI-cell initiation have also been noted in several species of apomictic *Hieracium* including *H. piloselloides* D18 (Koltunow *et al.*, 2000) and *H. aurantiacum* A36 (Koltunow *et al.*, 1998*b*). Based on the results of *GluB-1:RNase* expression, it seems likely that abnormal funiculus development in D18 contributes to the de-regulation of apomixis compared with D36 (Koltunow *et al.*, 2000). In terms of the apomictic process, this indicates that information restricting the number and position of AI cells relative to the sexual cells is dependent upon the integrity of sporophytic structures such as the funiculus and the receptacle.

The phenotypes observed in *GluB-1:RNase* ovules could be caused by a number of factors. These include the inhibition of signalling molecule synthesis or movement through the funiculus and/or general stress responses. Stress can take many forms in plants, including abiotic and biotic stimuli, both of which have pronounced effects on reproduction (Sun *et al.*, 2004; Oshino *et al.*, 2007). Reproductive stress has been associated with altered levels of hormones and downstream response pathways, including salicylic acid (Martinez *et al.*, 2004), jasmonic acid (Avanci *et al.*, 2010), and auxin (Jain and Khurana, 2009). Interestingly, alterations in apomictic development, including the precocious appearance of extra AI cells, could be induced by inhibiting polar auxin transport in flowers from apomictic *Hieracium* using NPA. In *Hieracium* plants containing DR5:GFP, which marks auxin accumulation, expression was noticeably absent from sexual and apomictic reproductive cells, but was detected in specific sporophytic regions of the ovule including the connective tissues of the funiculus, the tip of the growing nucellus, and the tip of the growing integument. Inhibition of polar auxin transport by NPA appeared to slow auxin flow away from these sites, since GFP fluorescence accumulated to higher levels in these regions and also in adjoining cells within 24 h of application. Although DR5:GFP expression increased dramatically in NPA-treated ovules, it is unclear whether altered levels of auxin in specific regions of the ovule, the slowed auxin flow out of the ovule or both contribute to the observed ovule phenotypes. Also, it is not clear whether the de-regulation of apomixis induced by altered auxin transport is directly due to changes in *LOA* activity or indirectly due to changes in ovule development. Irrespective, the results to date indicate that changes in auxin transport lead to the non-cell-autonomous de-regulation of the apomictic process. Similar to the *GluB-1:RNase* results, these changes were only induced in backgrounds containing *LOA*. Therefore, the initiation and progression of apomixis in *Hieracium* appears to depend upon the expression of *LOA* and the ability of sporophytic cells to respond to this information. The capacity of ovule cells to respond is directly or

indirectly regulated by funiculus growth and auxin transport, which appear to impart control on the apomictic process by restricting reproductive competence and potential (Fig. 5).

Piecing together factors that contribute to the progression of apomixis in Hieracium

In a recent study, a transgenic approach using *SPOROCYTELESS:RNase* determined that the meiotic events of megasporogenesis are required for the initiation of apospory in D36 (Koltunow *et al.*, 2011). Consistent with a close relationship between sexual processes and the initiation of apomixis, results from the current study show that even in severely deformed ovules, AI cells are only observed in ovules exhibiting some evidence of having initiated sexual reproduction. However, the results presented here showed that AI cells were observed prior to meiotic divisions of the MMC in *GluB-1:RNase* and NPA-treated D36 ovules. A similar observation was made in ectopic ovules from D36 plants transformed with *35S:rolB* (Koltunow *et al.*, 2001). One possibility is that the ovule defects induced by these treatments uncouple or prematurely induce programmes required for AI initiation that normally act downstream of megasporogenesis.

The reason for the increased number of AI cells detected in the *GluB-1:RNase* and NPA treated plants is uncertain. Studies in *Arabidopsis* have shown that signals from nucellar epidermal cells involving small RNAs and *ARGONAUTE9* are required to prevent sub-epidermal cells, other than the functional megaspore, from adopting gametophytic identity (Olmedo-Monfil *et al.*, 2010). This suggests that a lack of small RNA-mediated repression in *ago9* mutants leads to a broader zone of reproductive competence. It is possible that a similar mechanism might be indirectly compromised by the *Glub-1:RNase* and NPA treatments in *Hieracium* (Fig. 5), leading to the increased number and altered position of AI cells.

Despite an increased number of AI cells, aposporous embryo sac development was compromised in the most severely deformed ovules from *GluB-1:RNase* plants. This might relate to the failure of the integument to grow correctly and surround the nucellar lobe (Fig. 1B). NPA treatment also led to an inhibition of integument growth, but, by contrast, embryo sac development continued apparently independently of the surrounding tissues (Fig. 1C). A remarkably similar phenotype was noted in *Arabidopsis* ovules mis-expressing the *AUXIN RESPONSE FACTOR6* (*ARF6*) or *ARF8* transcription factors (Wu *et al.*, 2006). Combined with our NPA data, this indicates that, at certain

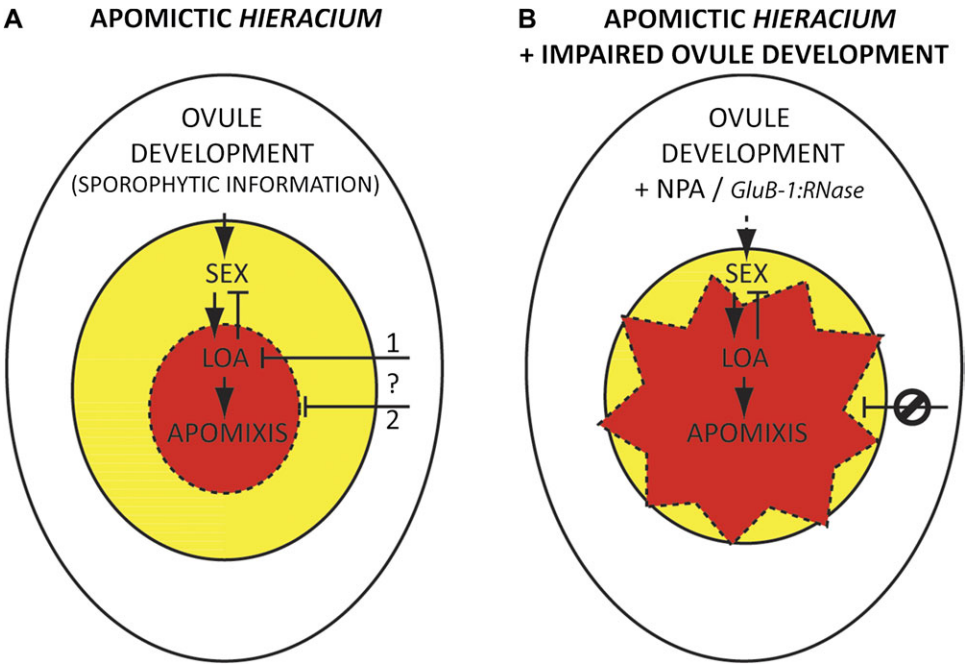

Fig. 5. Model for the interaction between ovule development and apomixis in *Hieracium*. (A) Initiation of apomixis in apomictic *Hieracium*. Sporophytic information (white ring), including polar auxin flow and funiculus growth, promotes normal development of ovule cells. This creates an environment suitable for the initiation and progression of megasporogenesis (SEX; inner yellow ring), and the subsequent stimulation of *LOSS OF APOMEIOSIS* (*LOA*) and AI formation (Koltunow *et al.*, 2011). Sporophytic information also ensures that *LOA* activity is directly (1) or indirectly (2) restricted to a limited zone of sporophytic cells (central red ring). (B) Ovule development in apomictic *Hieracium* after NPA or *GluB-1:RNase* treatment. Sporophytic information still acts to promote the development of ovule cells and induce sexual processes, albeit with decreased efficiency (dashed arrow and smaller yellow ring). The requirement for megasporogenesis to stimulate AI formation is partially compromised. A lack of spatial and temporal control from surrounding ovule cells means that a greater number of cells can respond to *LOA* and initiate apomictic development (convoluted red shape).

developmental stages, both sexual and aposporous embryo sac growth can continue independently of the surrounding ovule tissues.

The different ovule deformities and stresses reported here and previously show that apomixis is sensitive to a variety of inputs, but in most cases is a remarkably resilient process that leads to the formation of viable seed (Koltunow, 2000; Koltunow *et al.*, 2000, 2001; Rodrigues *et al.*, 2008). Apart from the actions of *LOA* and *LOP*, it appears that apomictic *Hieracium* utilizes the underlying sexual machinery to support apomictic events (Tucker *et al.*, 2003). However, it has remained unclear how control is imparted onto the apomictic process, restricting reproductive potential to one or a few sporophytic cells and ensuring that downstream events can occur in sequence. It seems likely that the stage-specific information from sexual cells and sporophytic ovule tissues is an important component of this process.

Acknowledgements

We thank Dolf Weijers for providing the DR5:GFP construct and Anne Tassie for assistance with transformations. We also thank Steve Swain, Paul Boss, three anonymous reviewers and members of the Koltunow laboratory for critical comments and helpful discussions. This work was supported by a DIISR Australia/India grant to AMK.

References

Avanci NC, Luche DD, Goldman GH, Goldman MH. 2010. Jasmonates are phytohormones with multiple functions, including plant defense and reproduction. *Genetic and Molecular Research* **9,** 484–505.

Balasubramanian S, Schneitz K. 2000. *NOZZLE* regulates proximal–distal pattern formation, cell proliferation and early sporogenesis during ovule development in *Arabidopsis thaliana*. *Development* **127,** 4227–4238.

Beals TP, Goldberg RB. 1997. A novel cell ablation strategy blocks tobacco anther dehiscence. *Plant Cell* **9,** 1527–1545.

Bencivenga S, Colombo L, Masiero S. 2011. Cross talk between the sporophyte and the megagametophyte during ovule development. *Sexual Plant Reproduction* **24,** 113–121.

Bicknell RA, Borst NK. 1994. *Agrobacterium*-mediated transformation of *Hieracium aurantiacum*. *International Journal of Plant Sciences* **155,** 467–470.

Catanach AS, Erasmuson SK, Podivinsky E, Jordan BR, Bicknell R. 2006. Deletion mapping of genetic regions associated with apomixis in *Hieracium*. *Proceedings of the National Academy of Sciences, USA* **103,** 18650–18655.

Chaudhury A, Koltunow A, Payne T, Luo M, Tucker M, Dennis E, Peacock W. 2001. Control of early seed development. *ANNUAL REVIEW OF CELL AND DEVELOPMENTAL BIOLOGY* **17,** 677–699.

Curtis MD, Grossniklaus U. 2007. Amphimixis and apomixis: two sides of the same coin? In: Hörandl E, Grossniklaus U, van Dijk PJ, Sharbel TF, eds. *Apomixis: evolution, mechanisms and perspectives*. Rugell, Liechtenstein: ARG Gantner Verlag, 37–62.

De Martinis D, Mariani C. 1999. Silencing gene expression of the ethylene-forming enzyme results in a reversible inhibition of ovule development in transgenic tobacco plants. *The Plant Cell* **11,** 1061–1072.

Dorcey E, Urbez C, Blazquez MA, Carbonell J, Perez-Amador MA. 2009. Fertilization-dependent auxin response in ovules triggers fruit development through the modulation of gibberellin metabolism in *Arabidopsis*. *The Plant Journal* **58,** 318–332.

Gasser CS, Broadhvest J, Hauser BA. 1998. Genetic analysis of ovule development. *Annual Review of Plant Physiology and Plant Molecular Biology* **49,** 1–24.

Goetz M, Vivian-Smith A, Johnson SD, Koltunow AM. 2006. *AUXIN RESPONSE FACTOR8* is a negative regulator of fruit initiation in Arabidopsis. *The Plant Cell* **18,** 1873–1886.

Gross-Hardt R, Lenhard M, Laux T. 2002. *WUSCHEL* signaling functions in interregional communication during *Arabidopsis* ovule development. *Genes and Development* **16,** 1129–1138.

Jain M, Khurana JP. 2009. Transcript profiling reveals diverse roles of auxin-responsive genes during reproductive development and abiotic stress in rice. *FEBS Journal* **276,** 3148–3162.

Kobayashi S, Ikeda I, Nakatani M. 1979. Studies on nucellar embryogenesis in citrus. 2. Formation of the primordium cell of the nucellar embryo in the ovule of the flower bud, and its meristematic activity. *Journal of the Japanese Society for Horticultural Science* **48,** 179–185.

Koltunow AM. 2000. The genetic and molecular analysis of apomixis in the model plant. *Hieracium. Acta Biologica Cracoviensia Series Botanica* **42,** 61–72.

Koltunow AM, Brennan P, Bond JE, Barker SJ. 1998*a*. Evaluation of genes to reduce seed size in Arabidopsis and tobacco and their application to Citrus. *Molecular Breeding* **4,** 235–251.

Koltunow AM, Grossniklaus U. 2003. Apomixis: a developmental perspective. *Annual Review of Plant Biology* **54,** 547–574.

Koltunow AM, Johnson SD, Bicknell RA. 2000. Apomixis is not developmentally conserved in related, genetically characterized *Hieracium* plants of varying ploidy. *Sexual Plant Reproduction* **12,** 253–266.

Koltunow AM, Johnson SD, Bicknell RA. 1998*b*. Sexual and apomictic development in *Hieracium*. *Sexual Plant Reproduction* **11,** 213–230.

Koltunow AM, Johnson SD, Lynch M, Yoshihara T, Costantino P. 2001. Expression of *rolB* in apomictic *Hieracium piloselloides* Vill. causes ectopic meristems *in planta* and changes in ovule formation, where apomixis initiates at higher frequency. *Planta* **214,** 196–205.

Koltunow AM, Johnson SD, Rodrigues JC, *et al*. 2011. Sexual reproduction is the default mode in apomictic *Hieracium* subgenus *Pilosella*, in which two dominant loci function to enable apomixis. *The Plant Journal* **66,** 890–902.

Koltunow AM, Soltys K, Nito N, McClure S. 1995. Anther, ovule seed, and nucellar embryo development in *Citrus sinensis* cv. Valencia. *Canadian Journal of Botany* **73,** 1567–1582.

Mariani C, Beuckeleer MD, Truettner J, Leemans J, Goldberg RB. 1990. Induction of male sterility by a chimaeric ribonuclease gene. *Nature* **347,** 737–741.

Martinez C, Pons E, Prats G, Leon J. 2004. Salicylic acid regulates flowering time and links defence responses and reproductive development. *The Plant Journal* **37,** 209–217.

Nemhauser JL, Feldman LJ, Zambryski PC. 2000. Auxin and *ETTIN* in *Arabidopsis* gynoecium morphogenesis. *Development* **127,** 3877–3888.

Ohashi-Ito K, Oda Y, Fukuda H. 2010. Arabidopsis *VASCULAR-RELATED NAC-DOMAIN6* directly regulates the genes that govern programmed cell death and secondary wall formation during xylem differentiation. *The Plant Cell* **22,** 3461–3473.

Okada T, Catanach A, Johnson S, Bicknell R, Koltunow A. 2007. An *Hieracium* mutant, *loss of apomeiosis* 1 (*loa1*) is defective in the initiation of apomixis. *Sexual Plant Reproduction* **20,** 199–211.

Okada T, Ito K, Johnson SD, Oelkers K, Suzuki G, Houben A, Mukai Y, Koltunow AM. 2011. Chromosomes carrying meiotic avoidance loci in three apomictic eudicot *Hieracium* subgenus *Pilosella* species share structural features with two monocot apomicts. *Plant Physiology* **157,** 1327–1341.

Olmedo-Monfil V, Duran-Figueroa N, Arteaga-Vazquez M, Demesa-Arevalo E, Autran D, Grimanelli D, Slotkin RK, Martienssen RA, Vielle-Calzada JP. 2010. Control of female gamete formation by a small RNA pathway in *Arabidopsis*. *Nature* **464,** 628–632.

Oshino T, Abiko M, Saito R, Ichiishi E, Endo M, Kawagishi-Kobayashi M, Higashitani A. 2007. Premature progression of anther early developmental programs accompanied by comprehensive alterations in transcription during high-temperature injury in barley plants. *Molecular Genetics and Genomics* **278,** 31–42.

Pagnussat GC, Alandete-Saez M, Bowman JL, Sundaresan V. 2009. Auxin-dependent patterning and gamete specification in the *Arabidopsis* female gametophyte. *Science* **324,** 1684–1689.

Reed RC, Brady SR, Muday GK. 1998. Inhibition of auxin movement from the shoot into the root inhibits lateral root development in *Arabidopsis*. *Plant Physiology* **118,** 1369–1378.

Reiser L, Modrusan Z, Margossian L, Samach A, Ohad N, Haughn GW, Fischer RL. 1995. The *BELL1* gene encodes a homeodomain protein involved in pattern formation in the *Arabidopsis* ovule primordium. *Cell* **83,** 735–742.

Rodrigues JC, Tucker MR, Johnson SD, Hrmova M, Koltunow AM. 2008. Sexual and apomictic seed formation in *Hieracium* requires the plant polycomb-group gene *FERTILIZATION INDEPENDENT ENDOSPERM*. *The Plant Cell* **20,** 2372–2386.

Schruff MC, Spielman M, Tiwari S, Adams S, Fenby N, Scott RJ. 2006. The *AUXIN RESPONSE FACTOR 2* gene of *Arabidopsis* links auxin signalling, cell division, and the size of seeds and other organs. *Development* **133,** 251–261.

Sun K, Hunt K, Hauser BA. 2004. Ovule abortion in *Arabidopsis* triggered by stress. *Plant Physiology* **135,** 2358–2367.

Takaiwa F, Yamanouchi U, Yoshihara T, Washida H, Tanabe F, Kato A, Yamada K. 1996. Characterization of common *cis*-regulatory elements responsible for the endosperm-specific expression of members of the rice glutelin multigene family. *Plant Molecular Biology* **30,** 1207–1221.

Tucker MR, Araujo AC, Paech NA, Hecht V, Schmidt ED, Rossell JB, De Vries SC, Koltunow AM. 2003. Sexual and apomictic reproduction in *Hieracium* subgenus *Pilosella* are closely interrelated developmental pathways. *The Plant Cell* **15,** 1524–1537.

Tucker MR, Koltunow AMG. 2009. Sexual and asexual (apomictic) seed development in flowering plants: molecular, morphological and evolutionary relationships. *Functional Plant Biology* **36,** 490–504.

Ulmasov T, Murfett J, Hagen G, Guilfoyle TJ. 1997. Aux/IAA proteins repress expression of reporter genes containing natural and highly active synthetic auxin response elements. *The Plant Cell* **9,** 1963–1971.

Villanueva J, Broadhvest J, Hauser B, Meister R, Schneitz K, Gasser C. 1999. *INNER NO OUTER* regulates abaxial–adaxial patterning in *Arabidopsis* ovules. *Genes and Development* **13,** 3160–3169.

Weijers D, Schlereth A, Ehrismann JS, Schwank G, Kientz M, Jurgens G. 2006. Auxin triggers transient local signaling for cell specification in *Arabidopsis* embryogenesis. *Developmental Cell* **10,** 265–270.

Wu CY, Suzuki A, Washida H, Takaiwa F. 1998. The GCN4 motif in a rice glutelin gene is essential for endosperm-specific gene expression and is activated by *Opaque-2* in transgenic rice plants. *The Plant Journal* **14,** 673–683.

Wu MF, Tian Q, Reed JW. 2006. Arabidopsis microRNA167 controls patterns of *ARF6* and *ARF8* expression, and regulates both female and male reproduction. *Development* **133,** 4211–4218.

Yang WC, Shi DQ, Chen YH. 2010. Female gametophyte development in flowering plants. *Annual Review of Plant Biology* **61,** 89–108.

Yang WC, Ye D, Xu J, Sundaresan V. 1999. The *SPOROCYTELESS* gene of *Arabidopsis* is required for initiation of sporogenesis and encodes a novel nuclear protein. *Genes and Development* **13,** 2108–2117.